Optics Communications 414 (2018) 172–176

Contents lists available at ScienceDirect

Optics Communications

journal homepage: www.elsevier.com/locate/optcom

# Unidirectional reflectionless propagation in non-Hermitian metamaterial based on phase coupling between two resonators

Hongda Yin [a], Ruiping Bai [a], Xintong Gu [a], Cong Zhang [a], Guang Rui Gu [a], Ying Qiao Zhang [a,*], Xing Ri Jin [a,*], YoungPak Lee [b]

[a] Department of Physics, College of Science, Yanbian University, Yanji, Jilin 133002, People's Republic of China
[b] Quantum Photonic Science Research Center and Department of Physics, Hanyang University, Seoul 133-791, Republic of Korea

ARTICLE INFO

*Keywords:*
Metamaterial
Resonator
Unidirectional reflectionlessness
Coherent perfect absorption

ABSTRACT

Unidirectional reflectionless propagation in a non-Hermitian metamaterial is obtained based on phase coupling between two resonators. The unidirectional reflectionless propagation can be obtained at exceptional point by adjusting polarization angle $\theta$ and distance $d$ between two resonators. Moreover, coherent prefect absorptions are obtained near exceptional point with the high absorbance of ~0.99 and high quality factor of ~83.



Parity-time (PT) symmetry has been extensively investigated in various of fields since it was proposed by Bender et al. [1,2]. Under PT symmetry, a non-Hermitian Hamiltonian can have the real eigenvalues. By far, PT optical materials have exhibited a variety of specific phenomena, such as single mode laser [3–6], coherent prefect absorber [7–9], optical comber filter [10], optical non-reciprocal propagation [11–17], unidirectional transmission [18,19], unidirectional reflectionlessness [20–33], and so on.

Recently, some attentions have been concentrated on investigating unidirectional reflectionless phenomenon based on balanced gain and loss [21–23]. More than that, unidirectional reflectionlessness has been investigated in non-Hermitian system without balanced gain and loss [24–27,30–32]. Feng et al. [24] demonstrated experimentally that an unidirectional reflectionless PT metamaterial could be obtained without gain at optical frequencies. They also realized unidirectional reflectionless light transport by a large-scale multilayer structure at visible frequencies experimentally [25]. Chang et al. [30] and Gu et al. [31] realized unidirectional reflectionlessness at exceptional point (EP) with quality factors ($Q$-factors) of ~15 and ~41 by using silver nanodisk and silver nanoring structures, respectively, based on Fabry–Pérot (FP) resonance coupling between two resonators. Further, Bai et al. [32] proposed a pair of silver crosses structure to achieve unidirectional reflectionlessness at EP with $Q$-factor of ~38.

In this paper, we investigated unidirectional reflectionlessness at EP in a non-Hermitian metamaterial system consisted of two-layered silicon (Si) resonators. The unidirectional reflectionless phenomenon at EP can be obtained by adjusting the polarization angle $\theta$ and distance $d$. Due to the low loss of Si, the resonators in our system have larger scales for the approximate resonant frequency and higher $Q$-factor compared with that in schemes [30–32].

The diagram of unit cell of the non-Hermitian metamaterial is shown in Fig. 1. A strip Si resonator and a disk Si resonator are completely embedded in photopolymer. The photopolymer layer is deposited on glass substrate. The conductivity and permittivity of Si are $2.5\times10^{-4}$ S/m and 11.9, respectively, and the permittivities of photopolymer and glass are 2.4025 (loss tangent 0.0077) and 2.25, respectively. The distance $d$ between two Si resonators is tunable. The numerical simulations are performed by a finite integration package (CST Microwave Studio). The boundary condition of system is the unit cell in $x$ and $y$ directions while is open in $z$ direction.

To corroborate the unidirectional reflectionless properties, we use scattering matrix method to illustrate the reflection spectra of the non-Hermitian system. The scatting properties for the metamaterial system in Fig. 1 can be expressed by transfer matrix $T_{all}$ [34–36] at a certain frequency $\omega$, as

$$T_{\mathrm{all}} = T_{\mathrm{s}}^{1} \times T_{\mathrm{p}} \times T_{\mathrm{s}}^{2} = \begin{pmatrix} T_{11} & T_{12} \\ T_{21} & T_{22} \end{pmatrix}, \quad (1)$$

$$T_{\mathrm{s}}^{1(2)} = \begin{pmatrix} 1 - \dfrac{i\gamma_{1(2)}}{\omega - \omega_{1(2)} + i\frac{\Gamma_{1(2)}}{2}} & \dfrac{-i\gamma_{1(2)}}{\omega - \omega_{1(2)} + i\frac{\Gamma_{1(2)}}{2}} \\ \dfrac{i\gamma_{1(2)}}{\omega - \omega_{1(2)} + i\frac{\Gamma_{1(2)}}{2}} & 1 + \dfrac{i\gamma_{1(2)}}{\omega - \omega_{1(2)} + i\frac{\Gamma_{1(2)}}{2}} \end{pmatrix}, \quad (2)$$

* Corresponding authors.
*E-mail addresses:* yqzhang@ybu.edu.cn (Y.Q. Zhang), xrjin@ybu.edu.cn (X.R. Jin).

https://doi.org/10.1016/j.optcom.2018.01.019
Received 11 November 2017; Received in revised form 1 January 2018; Accepted 11 January 2018
0030-4018/

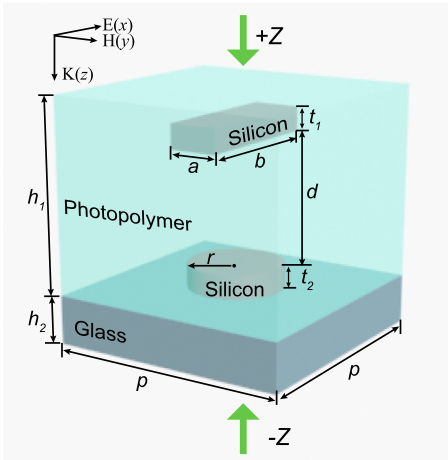


**Fig. 1.** Diagram of unit cell of the non-Hermitian metamaterial. The geometrical parameters are $a = 230$ nm, $b = 620$ nm, $t_1 = 165$ nm, $r = 235$ nm, $t_2 = 150$ nm, $h_2 = 300$ nm and $p = 900$ nm. The distance $d$ between two Si resonators is tunable, and $h_1$ varies with the change of $d$. The direction of incident wave is in $+z$ or $-z$.

and

$$T_p = \begin{pmatrix} \exp(i\phi) & 0 \\ 0 & \exp(-i\phi) \end{pmatrix}. \quad (3)$$

Here, $T_s^{1(2)}$ and $T_p$ are transfer matrices for Si strip (Si disk) and for the phase shift of the incident wave propagation between two resonators, respectively. $\omega$ and $\omega_{1(2)}$ are the incident wave frequency and resonant frequency of Si strip (Si disk), respectively. $\gamma_{1(2)}$ and $\Gamma_{1(2)}$ are the width of resonance and dissipative losses of Si strip (Si disk), respectively. $\phi$ is the accumulated phase shift for the incident wave propagation between two resonators.

Based on transfer matrix $T_{all}$, we can achieve the reflection and transmission coefficients [37] in both $+z$ and $-z$ directions, as

$$r_{+z} = \frac{-T_{21}}{T_{22}}, \quad r_{-z} = \frac{T_{12}}{T_{22}}, \quad t = t_{+z} = t_{-z} = \frac{1}{T_{22}}, \quad (4)$$

where $r_{+z}$ ($r_{-z}$) and $t_{+z}$ ($t_{-z}$) represent the reflection and transmission coefficients in $+z$ ($-z$) direction, respectively.

In order to illustrate the unidirectional reflectionless phenomenon clearly, we plot the simulated (solid lines) and analyzed (dot lines) reflection spectra in both $+z$ and $-z$ directions in Fig. 2. According to Fig. 2(a)–(c), there is a good agreement between the results of analytical calculation (dot lines) and numerical simulation (solid lines). Fig. 2(a) (2(c)) displays the reflection spectrum versus frequency for $d = 1184$ nm (1318 nm). From Fig. 2(a) (2(c)), unidirectional reflectionless phenomenon appears at EP 205.31 THz (202.25 THz)and the corresponding reflectances are ~ 0.004 (~0.818) and ~ 0.879 (~0) in $+z$ and $-z$ directions, respectively. Fig. 2(b) exhibits the identical reflectances for $d = 1260$ nm in $+z$ and $-z$ directions. Fig. 2(d) shows the corresponding fitted parameters $\Gamma_{1(2)}$ and $\gamma_{1(2)}$ versus the distance $d$ of 1184 nm, 1260 nm and 1318 nm, respectively. With the increase of $d$ from 1184 nm to 1318 nm, these parameters maintain a well stable trend. And Fig. 2(e) (2(f)) is the transmission spectrum with the transmittance of ~ 0.005 (~0.045) at 205.31 THz (202.25 THz).

To further analyze the unidirectional reflectionlessness at EP, we exhibit $z$-component distributions of electric field for two resonators in Fig. 3. In $+z$ direction, for $d=1184$ nm at 205.31 THz, Si strip resonator and Si disk resonator are both excited strongly. The induced currents are in the same directions as shown in Fig. 3(a) and (b), which means that the phase difference between two Si resonators is close to $2\pi$. Thus, the low reflectance (~0) occurs at EP based on FP resonance. Conversely, in $-z$ direction, the induced currents at 205.31 THz are in opposite directions as shown in Fig. 3(c) and (d). That is to say, the phase difference between two Si resonators is nearly $\pi$, resulting in the high reflectance (shown in Fig. 2(a)). And the case for $d = 1318$ nm at 202.25 THz in Fig. 3(e)–(h) is contrary to that of $d = 1184$ nm at 205.31 THz. From Fig. 3(e)–(h) the two resonators are strongly excited, and their induced currents are opposite and same in $+z$ and $-z$ directions, respectively. The corresponding phase differences between two resonators are ~ $\pi$ and ~ $2\pi$ in $+z$ and $-z$ directions, respectively. Therefore, the high reflectance and low reflectance occur in $+z$ and $-z$ directions at EP, respectively. Namely, unidirectional reflectionlessness is obtained at EP.

Furthermore, according to Eqs. (1) and (2), we can obtain the phase shift $\phi_{1(2)}$ for Si strip (disk) resonator [36], as

$$\phi_{1(2)} = \arctan\left[\frac{\mathrm{Im}(T_{s,21}^{1(2)}/T_{s,22}^{1(2)})}{\mathrm{Re}(T_{s,21}^{1(2)}/T_{s,22}^{1(2)})}\right] = \frac{(\omega-\omega_{1(2)})}{(\gamma_{1(2)}+\Gamma_{1(2)})}. \quad (5)$$

For our system, the phase difference $\phi_{all}$ between two resonators is composed of three parts: the phase shift for each Si resonator ($\phi_1$, $\phi_2$) and the phase shift propagating between two resonators ($\phi$). Thus, phase difference $\phi_{all}$ can be expressed as $\phi_{all} = \phi_1 - \phi_2 + 2\phi$ in $+z$ direction and $\phi_{all} = \phi_2 - \phi_1 + 2\phi$ in $-z$ direction. According to Eq. (5) and some relevant parameters, we obtain that $\phi_{all}$ is ~ $2\pi$ in $+z$ direction at EP (205.31 THz), resulting in reflectance is ~ 0 based on the Fabry–Pérot resonant coupling (Fig. 2(a)). For another EP (202.25 THz), $\phi_{all}$ is ~ $2\pi$ in $-z$ direction and the corresponding reflectance is ~ 0 (Fig. 2(c)).

Fig. 4 shows the reflection spectra and $z$-component distributions of electric field when electric field of incident wave is parallel to $x$ direction (polarization angle $\theta = 0°$) or $y$ direction (polarization angle $\theta = 90°$), respectively. From Fig. 4(a), unidirectional reflectionlessness can be obtained by adjusting polarization angle of the incident wave. When $\theta = 0°$, the reflectance is ~ 0, while when $\theta = 90°$, the reflectance is ~ 0.77 at 205.31 THz. From Fig. 4(b), both two resonators are excited by incident wave at $\theta = 0°$ and their phase difference is ~ $2\pi$. The corresponding reflectance is ~ 0. And when $\theta = 90°$, only the Si disk resonator is excited by incident wave. In this case, the high reflectance appears.

Then we demonstrate the physical properties of the non-Hermitian system. According to Eq. (4), the scattering matrix $S$ can be described as

$$S = \begin{pmatrix} t & r_{-z} \\ r_{+z} & t \end{pmatrix}, \quad (6)$$

and the eigenvalues of the scatting matrix $S$ can be written as

$$\lambda_{1(2)} = t \pm \sqrt{r_{+z}r_{-z}}. \quad (7)$$

When $r_{+z}$ or $r_{-z}$ is zero, two eigenvalues coalesce and EP appears. At the EP, unidirectional reflectionlessness occurs. In order to describe the phenomenon in detail, we plot the real and imaginary parts of the eigenvalues $\lambda_1$, $\lambda_2$ for $\phi = 0.914\pi$, $\pi$ and $1.1\pi$, respectively, in Fig. 5. From Fig. 5(a) and (b) (5(e) and (f)), two real parts of the eigenvalues $\lambda_1$, $\lambda_2$ coalesce and two imaginary parts cross at 205.31 THz (202.25 THz) for $\phi = 0.914\pi$ ($\phi = 1.1\pi$), which indicates that EP occurs at 205.31 THz (202.25 THz). At the two EPs, unidirectional reflectionlessness is achieved, respectively, by adjusting the phase shift $\phi$. From Fig. 5(c) and (d), the real parts of $\lambda_1$ and $\lambda_2$ are separated and their imaginary parts intersect at zero point at 202.3 THz, 203.58 THz, and 205.87 THz, respectively. At these cross points, the eigenvalues of system are real, and $t$ and $\sqrt{r_{+z}r_{-z}}$ are both real. In this condition, our system is Hermitian. Beyond these cross points, one eigenvalue is real and the other is complex, and $t$ and $\sqrt{r_{+z}r_{-z}}$ are both complex.

In addition, coherent prefect absorptions (CPAs) [9] are obtained near EP as shown in Fig. 5(b) and (f) when one eigenvalue is real and the other is complex. Due to the reflectance (Fig. 2(a)) and transmittance (Fig. 2(e)) approach zero, both absorbances of CPAs at 205.26 THz and 205.36 THz are ~ 0.99 by formula $A = 1 - R - T$. And the corresponding $Q$-factors are ~ 83. Also, at 202.2 THz and 202.3 THz